Microwave-magnetic-field-induced magnetization excitation and assisted switching of antiferromagnetically coupled magnetic bilayer with perpendicular magnetization

Microwave-magnetic-field-induced magnetization excitation and assisted switching of antiferromagnetically coupled magnetic bilayer with perpendicular magnetization (F)

Hirofumi Suto, Taro Kanao (ID), Tazumi Nagasawa, Koichi Mizushima, Rie Sato (ID), Nobuaki Kikuchi, and
Satoshi Okamoto

COLLECTIONS

(F) This paper was selected as Featured

View Online   Export Citation   CrossMark

ARTICLES YOU MAY BE INTERESTED IN

Inducing out-of-plane precession of magnetization for microwave-assisted magnetic
recording with an oscillating polarizer in a spin-torque oscillator
Applied Physics Letters 114, 172403 (2019); https://doi.org/10.1063/1.5086476

Tomorrow's micromagnetic simulations
Journal of Applied Physics 125, 180901 (2019); https://doi.org/10.1063/1.5093730

The design and verification of MuMax3
AIP Advances 4, 107133 (2014); https://doi.org/10.1063/1.4899186

Microwave-magnetic-field-induced magnetization excitation and assisted switching of antiferromagnetically coupled magnetic bilayer with perpendicular magnetization ⓕ

Hirofumi Suto,[1,a)] Taro Kanao,[1] ⓘ Tazumi Nagasawa,[1] Koichi Mizushima,[1] Rie Sato,[1] ⓘ Nobuaki Kikuchi,[2] and Satoshi Okamoto[2]

AFFILIATIONS

[1]Corporate Research and Development Center, Toshiba Corporation, 1, Komukai-Toshiba-cho, Saiwai-ku, Kawasaki 212-8582, Japan
[2]Institute of Multidisciplinary Research for Advanced Materials, Tohoku University, Katahira 2-1-1, Aoba-ku, Sendai 980-8577, Japan

a)Author to whom correspondence should be addressed: hirofumi.suto@toshiba.co.jp

ABSTRACT

Antiferromagnetically coupled (AFC) magnetic bilayer is a candidate media structure for high-density magnetic recording. Because the stray fields from the two magnetic layers of the AFC bilayer cancel each other out, switching field distribution originating from the stray fields from the adjacent data bits can be suppressed. Furthermore, in microwave-assisted magnetic recording (MAMR), which utilizes ferromagnetic resonance (FMR) excitation in a microwave field to reverse a high-anisotropy magnetic material, AFC media can suppress the distribution in FMR frequency originating from the stray fields and improve MAMR performance. In this study, we fabricate an AFC magnetic bilayer consisting of two Co/Pt multilayers with perpendicular magnetization. We use anomalous-Hall-effect-FMR in combination with a circularly polarized microwave field and carry out layer-selective analysis of FMR excitation of the two magnetic layers. We then investigate the switching behavior of an AFC bilayer nanodot in a microwave magnetic field. The switching field decreases with increasing microwave field frequency and increases abruptly at the critical frequency, and a large switching field reduction by applying a microwave field is demonstrated. This switching behavior is similar to that of a single-layer perpendicular magnetic nanodot, showing that the AFC structure does not hinder the microwave assist effect.

Published under license by AIP Publishing. https://doi.org/10.1063/1.5089799

I. INTRODUCTION

In magnetic recording media, magnetic grains interact through stray fields. This dipolar interaction results in a switching field distribution because the switching condition of a magnetic grain is determined not only by the write field from the head element, but also by the stray fields from the adjacent grains. Dipolar interaction of media causes another issue in microwave-assisted magnetic recording (MAMR), which has been explored for next-generation magnetic recording.[1–16] MAMR uses a spin-torque oscillator (STO) integrated in a head element to generate a microwave magnetic field, which induces ferromagnetic resonance (FMR) excitation of media magnetization to assist reversing a high-anisotropy media material. Therefore,

matching between the FMR frequency and microwave field frequency is crucial. However, dipolar interaction leads to a distribution in media FMR frequency, which degrades the microwave assist efficiency.

Antiferromagnetically coupled (AFC) media have been shown to be effective for reducing dipolar interaction.[11,12,16–21] The simplest AFC media consists of two magnetic layers with a nonmagnetic layer between them. The nonmagnetic layer is usually composed of Ru or Ir and induces antiferromagnetic coupling between the two magnetic layers.[22,23] One magnetic layer is thicker or has a higher anisotropy than the other layer and maintains magnetization direction to stores data. The other layer is designed to reverse spontaneously by the

antiferromagnetic coupling and form an antiferromagnetic configuration in the remanent state. Because the stray fields from the two magnetic layers cancel out, AFC media can suppress dipolar interaction. AFC media was put into practical use in longitudinal recording,[17,18] and perpendicular AFC media have been studied for perpendicular recording.[19–21] The fabrication of CoCrPt-based AFC granular media with perpendicular magnetization has been reported, which showed that insertion of a thin Ru layer does not disturb the granular structure.[11] Recording simulation demonstrated a higher signal-to-noise ratio when AFC media are used for MAMR.[12]

We would also like to comment on the application of AFC media to multilayer recording in which media have vertically stacked multiple recording layers. It has been proposed that MAMR can perform layer-selective write when each recording layer is designed to have a different FMR frequency and the frequency of the microwave field is tuned to excite a target recording layer.[12–16] In multilayer recording, suppression of dipolar interaction by the use of AFC media is more crucial because of additional dipolar interaction between different recording layers. Note the following. Although the AFC structure consists of two magnetic layers, it represents one bit because only one layer acts as a storage layer, while the other layer suppresses the stray field. Multiple AFC structures are necessary for multi-layer recording.

There are concerns over read operation in AFC media. When a magnetoresistive read head that detects the stray field from media is used, the output amplitude from AFC media decreases because of the small stray field. To overcome this problem, a read method that detects FMR excitation of the media magnetization has been proposed.[24–26] This read method can be applied to layer-selective read in multilayer recording when FMR excitation of a target recording layer is induced by tuning the microwave field frequency.[27] The layer-selective write and read share the same principle in which a layer is selected in the frequency domain.

In this study, we investigate magnetization excitation and switching of an antiferromagnetically coupled magnetic bilayer in a microwave magnetic field. The bilayer consists of a hard magnetic layer (HL), a soft magnetic layer (SL), and a Ru layer between them. Both HL and SL are composed of a Co/Pt multilayer, and HL has a higher anisotropy than SL. A perpendicular antiferromagnetic magnetization configuration is formed in the remanent state because the antiferromagnetic coupling field acting on SL is higher than its anisotropy field. We study FMR excitation of the AFC bilayer dot by using the anomalous-Hall-effect (AHE)-FMR measurement developed by Kikuchi et al.[28] in combination with a circularly polarized microwave field. This method can selectively analyze the magnetic properties of the two magnetic layers, because magnetization excitation is induced when the frequency and rotation direction of the microwave field match the FMR frequency and precession direction of the magnetic layer. We then study microwave-assisted magnetization switching (MAS) behavior using an AFC bilayer nanodot. We use linearly and circularly polarized microwave fields. The microwave field polarization depends on the position of the media magnetization relative to the STO, and its effect on MAS is important in recording application. The switching field decreases almost linearly with increasing microwave field frequency, which is similar to the MAS behavior obtained for a single-layer perpendicular magnetic nanodot.[5,6,8] A larger MAS effect is obtained for the circularly

polarized microwave field, and the switching field substantially decreases from approximately 4 kOe to 1 kOe. It is also shown that the MAS effect is enhanced by a microwave field with time-varying frequency. This result demonstrates that a large MAS effect can be obtained for an AFC bilayer, showing that the combination of MAS and AFC media is a promising candidate technology for future high-density magnetic recording.

II. EXPERIMENT AND SIMULATION

Figure 1(a) shows the film structure of an AFC bilayer. Ta and Pt bottom layers, two Co/Pt magnetic multilayers with insertion of a Ru layer, and Pt and Ta capping layers are deposited on a sapphire substrate by using a magnetron sputtering system. The lower magnetic layer is HL and the upper magnetic layer is SL. HL is designed to have a higher anisotropy than SL by changing the Co/Pt thicknesses. We are unable to clearly measure the FMR frequency of this film by vector-network-analyzer (VNA)-FMR measurement because the magnetic layers are very thin. To estimate the
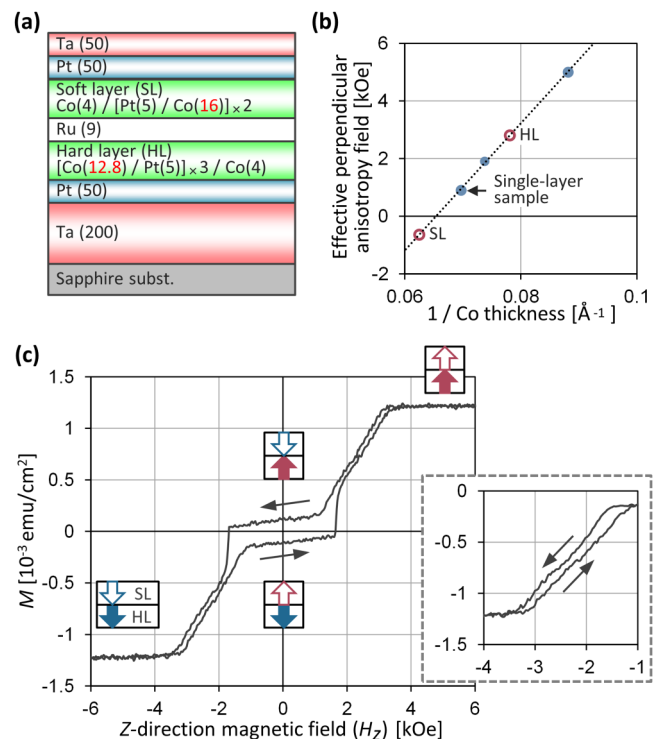

FIG. 1. (a) Film structure consisting of two antiferromagnetically coupled Co/Pt multilayers. Thicknesses are given in angstroms. (b) Effective anisotropy field vs inverse thickness of the Co layer (t_{Co}). Filled circles are the values estimated from the VNA-FMR measurement data for Ta 200/Pt 50/(Co t_{Co}/Pt 5) × 5/Pt 50/Ta 50 (from bottom to top, thicknesses given in angstroms). Open circles are the estimated values for HL and SL of the AFC bilayer. (c) M-H_z loop obtained for the film sample with an area of 1 × 1 cm². Schematics depict the magnetization configuration of the AFC bilayer. The inset shows a minor loop of SL switching.

anisotropy of the bilayer, we measure the VNA-FMR spectra of three kinds of single-layer Co/Pt multilayer films with five repeated sets of Co and Pt layers. Figure 1(b) shows the estimated effective anisotropy field including the demagnetizing field. From linear fitting, the effective anisotropy fields of HL and SL are estimated to be +2.8 kOe and −0.6 kOe, respectively. These estimates mean that HL intrinsically has perpendicular magnetization while SL intrinsically has in-plane magnetization. Figure 1(c) shows the perpendicular M-H loop measured by a vibrating sample magnetometer (VSM). When a z-direction magnetic field (H_z) of −6 kOe is applied, both HL and SL magnetizations are in the –z direction. As H_z increases, the SL magnetization gradually changes to the +z direction from −3.2 kOe to −1.2 kOe. The field width of the SL switching indicates that the effective anisotropy field of SL is −1 kOe, which roughly agrees with the value estimated from the VNA-FMR measurement. Because of the antiferromagnetic coupling, H_z of the SL switching is shifted, and the coupling field is estimated to be 2.2 kOe from the center of the minor loop [Fig. 1(c) inset]. At $H_z = 0$ kOe, HL and SL have a perpendicular antiferromagnetic configuration because the antiferromagnetic coupling field is large enough to make the SL magnetization in the perpendicular direction. The abrupt change at $H_z = +1.6$ kOe corresponds to the HL switching. After the abrupt change, the M-H curve almost agrees with that of the downward sweep. Considering that the whole HL magnetization is in the +z direction in the downward sweep, this agreement indicates that the whole HL magnetization reverses at $H_z = +1.6$ kOe. After the HL switching, the SL magnetization tilts from the +z direction because of the antiferromagnetic coupling. As H_z further increases to 3.3 kOe, the SL magnetization again saturates in the +z direction.

Figure 2 shows the sample structure and the measurement setup. The AFC bilayer film is patterned into a rectangular dot with a side of 500 nm and a circular dot with a diameter of 80 nm by electron-beam lithography and Ar ion milling. These samples
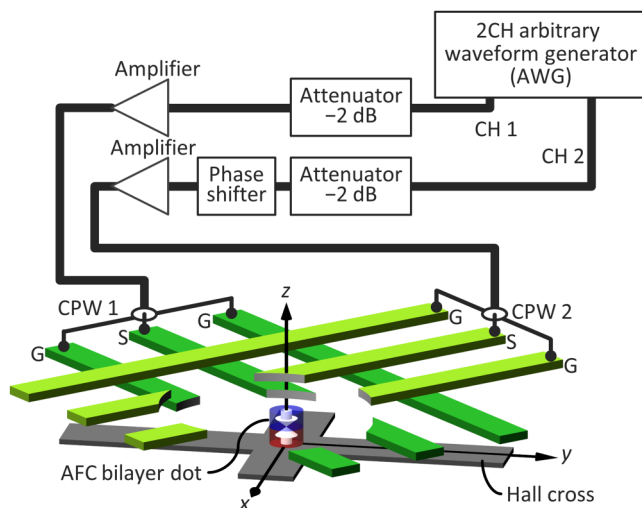

FIG. 2. Sample structure and experimental setup. Parts of the CPWs overlapping the AFC bilayer dot are not shown.

are used for FMR measurement and MAS measurement, respectively. The bottom layers are patterned into a Hall cross. Above the AFC bilayer dot, a 100-nm-thick insulating layer and a 100-nm-thick metal layer composed of Cu with thin adhesion layers are sputter-deposited. The metal layer is patterned into a coplanar waveguide (CPW) having a 1-μm-wide signal (S) line and two 2-μm-wide ground (G) lines. On the CPW, a 100-nm-thick insulating layer and a 100-nm-thick metal layer composed of Au with thin adhesion layers are sputter deposited. The second metal layer is also patterned into a CPW with the same dimension. The upper CPW is rotated by 90° with respect to the lower CPW in the x-y planes, so that they cross at a right angle above the AFC bilayer dot. The alignment accuracy of the AFC dot and the CPWs is within approximately 200 nm.

Two kinds of magnetic field are applied to the AFC bilayer dot: a z-direction magnetic field from an external electromagnet and an in-plane microwave magnetic field. The microwave field is generated by introducing microwave signals to the CPWs using the measurement setup shown in Fig. 2. The delay between the microwave signals in the two CPWs is controlled by changing the microwave waveforms from the arbitrary waveform generator (AWG) and changing the delay of the phase shifter. When the delay is 90°, a circularly polarized microwave field is generated, and the rotation direction of the microwave field can be reversed by changing the sign of the delay. The delay is adjusted as follows. The switching field of the magnetic dot is measured by applying 10 GHz microwave fields from both CPWs and by sweeping the delay. The dependence of the switching field on the delay shows the minimum, where the microwave field is closest to circular polarization. In the delay sweep, the delay is increased in steps of 3.125 ps, which corresponds to 1/32 of one period at 10 GHz. In AHE-FMR measurements, the microwave field is applied continuously, and in MAS measurements the microwave field is pulse-modulated to pulses with 10-ns plateau time with 5-ns rise and fall time and is applied repeatedly at 122 kHz to avoid temperature rise.

We also fabricate a similar sample using a single-layer perpendicular magnetic dot with a diameter of 80 nm for comparison. The single-layer perpendicular magnetic dot is patterned from the magnetic film having Ta 200/Pt 50/(Co 14.3/Pt 6) × 5/Pt 50/Ta 50 (from bottom to top, thicknesses given in angstroms). The effective anisotropy field of this film is +0.9 kOe, as shown in Fig. 1(b).

Micromagnetic simulation based on the Landau-Lifshitz-Gilbert equation is carried out using MuMax3 software.[29] The simulation parameters are shown in Table I. The parameters are derived from the VNA-FMR and VSM measurements. The model is a 500-nm circular dot for AHE-FMR simulation and an 80-nm circular dot for MAS simulation. The shape of the model for AHE-FMR simulation is different from the square dot used in the experiment. However, in AHE-FMR simulations, we consider only the main FMR signals corresponding to a uniform mode, and thus, neglect the difference in the shape. The models are divided into $2 \times 2 \times 5$ nm^3 cells.

III. RESULTS AND DISCUSSION

In this section, we first analyze the magnetic property of the AFC bilayer by AHE-FMR measurement in combination with a circularly polarized microwave field. We then investigate the switching behavior of the AFC bilayer nanodot by applying three kinds of

TABLE I. Simulation parameters.

Layer	Thickness (nm)	Saturation magnetization (emu/cm^3)	Damping constant	Perpendicular anisotropy (erg/cm^3)	Interlayer coupling (erg/cm^2)
Soft layer (SL)	5	1000	0.05	6×10^6	−1
Hard layer (HL)	5	1000	0.05	8×10^6	

microwave field: a linearly polarized microwave field, a circularly polarized microwave field, and a circularly polarized microwave field with time-varying frequency. We also investigate the MAS behavior of a single-layer perpendicular magnetic nanodot for comparison.

A. Anomalous-hall-effect-FMR measurement of an AFC magnetic bilayer (500nm rectangular dot) in a circularly polarized microwave field

Figure 3 shows AHE voltage vs H_z. The measured voltage is the sum of the AHE voltage from HL and SL, which is proportional to the z-direction component of the HL and SL magnetizations, respectively. In this experiment, AHE voltage is more sensitive to the HL magnetization because of the composition of the magnetic layer and the current flow. This result is similar to the VSM data [Fig. 1(c)], and shows the same magnetic configuration: with increasing H_z, the SL magnetization gradually changes to the $+z$ direction from approximately −2.5 kOe to −1 kOe and forms a perpendicular antiferromagnetic configuration in the remanent state. The switching field of the HL (H_{sw}) is +2.6 kOe, which is higher than that in the VSM data because patterning the film into the submicron dot reduces the nucleation sites. The patterning also changes the demagnetizing field and increases the effective anisotropy.
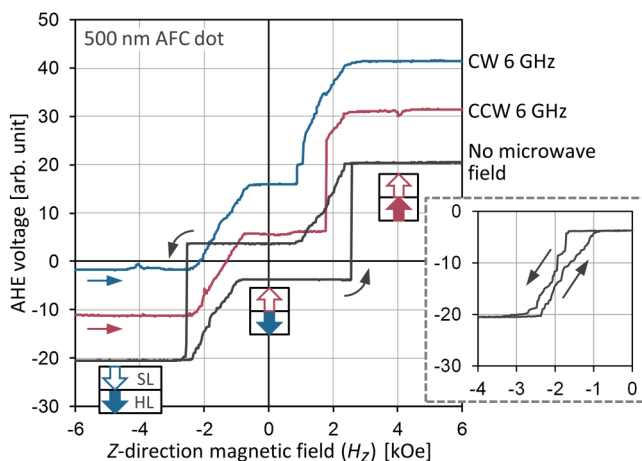

FIG. 3. AHE voltage vs H_z obtained for the 500-nm AFC bilayer dot. The three datasets are measured without microwave field and by applying CCW and CW 6 GHz microwave fields with H_{rf} of 213 Oe. Data are offset for clarity, and schematics depict the magnetization configuration. The inset shows a minor loop of SL switching without microwave field.

Figure 3 also shows AHE voltage vs H_z obtained by applying a continuous counterclockwise (CCW) microwave field with a frequency (f_{rf}) of 6 GHz and an amplitude (H_{rf}) of 213 Oe. Small dips appear at $H_z = 0$ kOe and +4 kOe. These dips indicate a decrease in the z-direction magnetization and are due to the FMR excitation, as explained below. When the CCW microwave field is applied to magnetization in the $+z$ direction at the FMR frequency, the magnetization starts to rotate around the $+z$ direction, and consequently, the z-direction component of the magnetization decreases. At around $H_z = 0$ kOe, the HL and SL magnetizations are in the $−z$ and $+z$ direction, respectively, and thus, the FMR signal originates from the SL excitation. At around $H_z = +4$ kOe, both HL and SL magnetizations are in the $+z$ direction. Judging from the frequency, the FMR signal originates from the SL excitation. Note that HL or SL excitation means that the HL or SL magnetization is mainly excited, while at the same time, the other layer is also excited because of the coupling. HL reverses at $H_z = +1.8$ kOe. This H_{sw} is smaller than that without microwave fields because of the temperature rise caused by applying the microwave signal. In addition, the microwave field has a small amount of clockwise (CW) component because the polarization not perfectly circular, and the CW component is expected to affects H_{sw} through the HL excitation. The details of a CW microwave field is discussed below.

When the rotation direction is reversed to CW, the magnetization in the $−z$ direction is excited, and a small peak due to FMR excitation appears at $H_z = −4$ kOe. This FMR signal is symmetric to the one at $H_z = +4$ kOe for the CCW microwave field and originates from the SL excitation. At $H_z = +0.8$ kOe, an abrupt change due to HL switching appears. This result indicates that MAS of HL occurs as a result of the HL excitation. To be precise, the change of the AHE voltage consists of multiple steps, showing that a part of the HL magnetization first reverses and then the whole HL magnetization reverses as the reversed domain expands.

Next, we investigate the FMR signals and MAS in more detail by changing f_{rf}. Figure 4(a) shows AHE voltage vs H_z in the H_z range from −6 kOe to −2 kOe for $f_{rf} = 4$, 6, 8, 10, 18, and 20 GHz. In this H_z range, both HL and SL magnetizations are in the $−z$ direction except for near $H_z = −2$ kOe, where the SL magnetization starts to reverse. The FMR signals are observed only for the CW microwave fields because of the rotation direction matching. As f_{rf} increases from 4 GHz, the SL FMR signal moves to the lower H_z side because decreasing H_z increases the effective field acting on SL with the magnetization in the $−z$ direction and accordingly increases the FMR frequency. Because H_{rf} is large, the magnetization excitation is in the nonlinear regime. Therefore, the shape of the FMR signal is asymmetric with a steeper slope at the higher H_z side. Furthermore, weak signals due to higher-order FMR modes are observed in the higher H_z side of the main signal. At $f_{rf} = 18$ GHz, another FMR signal appears, which originates from the HL
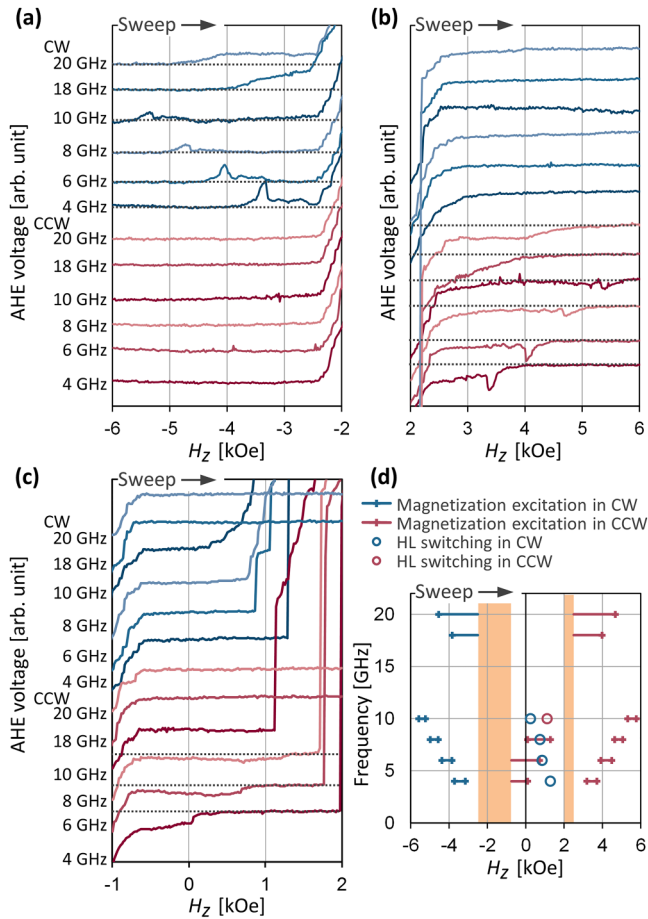
FIG. 4. (a)–(c) AHE voltage vs H_z obtained for the 500-nm AFC bilayer dot. The twelve datasets are measured by applying CCW and CW microwave fields with f_{rf} of 4, 6, 8, 10, 18, and 20 GHz and H_{rf} of 213 Oe. Dotted lines are a guide for emphasizing the FMR signals. Data are offset for clarity. (d) FMR signal linewidth and MAS condition plotted on the frequency vs H_z plane. The hatched regions represent the H_z range where the SL magnetization is in neither the +z nor −z direction. In this region, the linewidth of the FMR signals cannot be determined.

excitation and is broader than the SL excitation. The different linewidth is consistent with the theory of FMR: the higher FMR frequency indicates a higher effective field acting on the magnetic layer and the FMR linewidth is proportional to the effective field multiplied by the damping of the magnetic layer.[30] Figure 4(b) shows AHE voltage vs H_z in the H_z range from +2 kOe to +6 kOe, in which both the HL and SL magnetizations are mostly in the +z direction. The FMR signals are observed only for the CCW microwave fields, and the result is almost symmetric to Fig. 4(a).

Figure 4(c) shows AHE voltage vs H_z in the H_z range from −1 kOe to +2 kOe. As H_z increases from −1 kOe, the SL magnetization changes to the +z direction and forms an antiferromagnetic configuration. For the CCW microwave fields, the dip originating

from the SL excitation gradually moves to higher H_z as f_{rf} increases from 4 GHz to 8 GHz. The linewidth of the FMR signals in the antiferromagnetic configuration is broader than that in the ferromagnetic configuration [Fig. 4(b)] when compared at the same f_{rf}. The broader linewidth for the same f_{rf} suggests that the effective damping is larger in the antiferromagnetic configuration. At f_{rf} = 10 GHz, an abrupt change due to HL switching appears instead of an FMR signal. This H_{sw} is on the trend of the $f_{rf} - H_z$ relation of the SL FMR signals, indicating that the HL switching is induced by the SL excitation. This HL switching is probably caused by the following two reasons. The HL magnetization is indirectly excited by the SL excitation. The z-direction antiferromagnetic coupling field acting on HL decreases because the z-direction component of the SL magnetization decreases when the SL magnetization is excited. At f_{rf} = 18 and 20 GHz, no FMR signal is observed because the frequency is much higher than the SL FMR frequency.

For the CW microwave fields, microwave-assisted H_{sw} gradually decreases as f_{rf} increases from 4 GHz to 10 GHz. This result is consistent with the fact that HL is in the −z direction and its resonance H_z decreases as f_{rf} increases. At f_{rf} = 18 and 20 GHz, no MAS is obtained because the frequency is much higher than the HL FMR frequency.

Figure 4(d) summarizes the relation between f_{rf} and H_z regarding the FMR signals and MAS observed in Figs. 4(a)–4(c). The FMR signals and the microwave-assisted H_{sw} show an almost linear relation. Note that the ranges of the FMR signals are shown as a guide. The exact linewidth cannot be determined because the FMR signals are in the nonlinear regime and asymmetric and have higher-order signals in the vicinity. In the hatched regions, the SL magnetization is in neither the +z nor −z direction, and when the FMR signals overlap these regions, the linewidth of the FMR signals cannot be determined.

We carry out zero-temperature micromagnetic simulation to analyze the experimental data. Figure 5(a) shows the normalized z-component magnetization ($0.6 \times m_z^{HL} + 0.4 \times m_z^{SL}$) vs H_z. The ratio of HL and SL is set to reproduce the experimentally obtained AHE voltage-H_z data. Without microwave fields, the simulation result agrees with the experimental result except that H_{sw} is larger than that in the experiment. This is because the switching of HL is induced by thermal fluctuation in the experiment. In a CCW microwave field, two FMR signals appear at H_z = +1.5 kOe and +5.5 kOe with one in the antiferromagnetic configuration and the other in the ferromagnetic configuration. In a CW microwave field, MAS of the HL occurs at H_z = +1.8 kOe. These FMR signals and MAS qualitatively agree with the experimental results.

Figure 5(b) shows the normalized z-component magnetization of the HL and SL in the H_z range from +1 kOe to +5 kOe. In the CCW microwave field, the SL excitation is induced. In this condition, the HL magnetization is also slightly excited. In the CW microwave field, the whole HL magnetization reverses at H_z = 1.9 kOe owing to microwave assist, and accordingly the SL magnetization tilts from the +z direction because of the antiferromagnetic coupling. As H_z further increases, the SL magnetization again saturates in the +z direction.

Figure 5(c) shows the normalized z-component magnetization of HL and SL in the H_z range from +4 kOe to +8 kOe for 8 GHz and 26 GHz CCW microwave fields. At f_{rf} = 8 GHz, SL is mainly
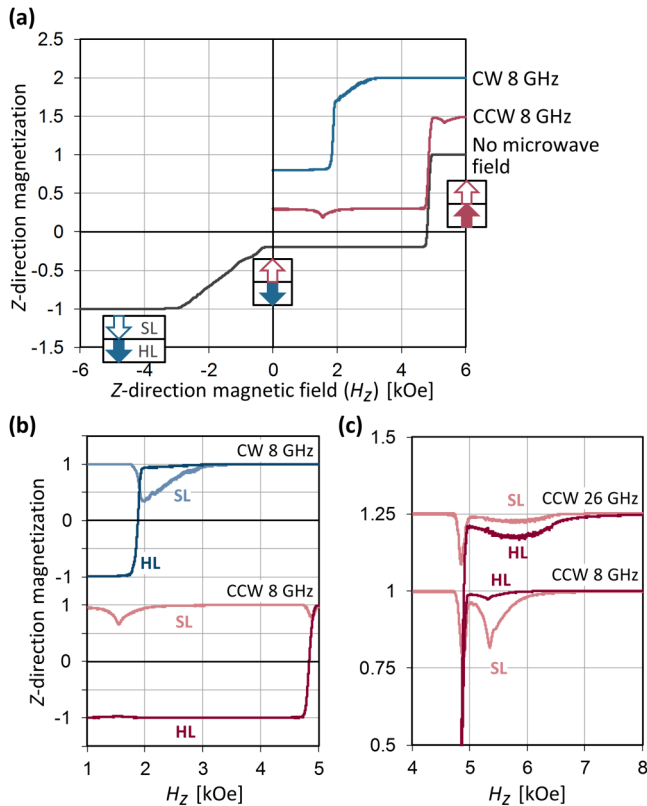
(a) **(b)** **(c)**

FIG. 5. (a) Computed normalized z-component magnetization ($0.6 \times m_z^{HL} + 0.4 \times m_z^{SL}$) vs H_z. The three datasets are obtained without microwave field and in CCW and CW 8 GHz microwave fields with H_{rf} of 200 Oe. Schematics depict the magnetization configuration. (b) and (c) Computed normalized z-component magnetization of HL and SL (b) in CCW and CW 8 GHz microwave fields with H_{rf} of 200 Oe and (c) in CCW 8 GHz and 26 GHz microwave fields with H_{rf} of 200 Oe. Data are offset for clarity.

FIG. 6. AHE voltage vs H_z obtained for the 80-nm AFC bilayer dot. Schematics depict the magnetization configuration.

excited, and at $f_{rf} = 26$ GHz, HL is mainly excited. The linewidth of the HL FMR is larger, which agrees with the experimental results. However, when the two FMR signals for the CCW 8 GHz in Figs. 5(b) and 5(c) are compared, they show similar linewidth, which does not agree with the experimental results in which the linewidth is broader in the antiferromagnetic configuration. This disagreement indicates that the effective damping of the bilayer increases in the antiferromagnetic configuration because of an effect that is not included in the micromagnetic simulation, such as local thickness variation of the Ru layer[31] and the spin pumping effect.[32]

B. Microwave-assisted magnetization switching of an AFC magnetic bilayer dot (80 nm circular dot)

Figure 6 shows AHE voltage vs H_z. Because the sample diameter of 80 nm is smaller than that used in the AHE-FMR measurement, SL has intrinsically perpendicular magnetization. As H_z increases from −5 kOe, SL reverses at $H_z = −0.2$ kOe and a perpendicular antiferromagnetic configuration is realized in the remant state, and
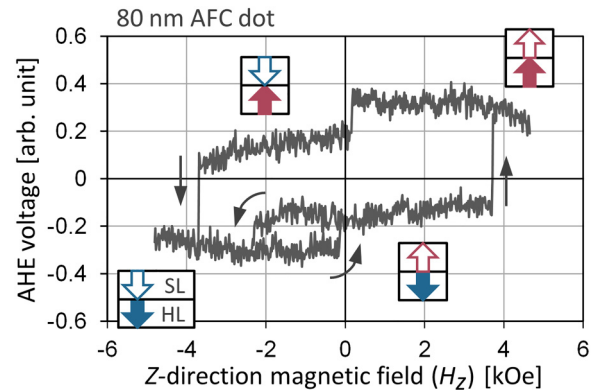
then HL reverses at +3.7 kOe. The AHE voltage has a larger ratio of the HL magnetization than in the AHE-FMR measurements because the current introduced from the bottom layers flows more preferentially in HL because of the smaller sample size.

Now, we focus on the switching of HL from the antiferromagnetic configuration and study MAS behavior by applying a microwave field. Figure 7(a) shows H_{sw} vs f_{rf} when a linearly polarized microwave field is generated by introducing a microwave signal to only the lower CPW. As f_{rf} increases, H_{sw} decreases almost linearly, becomes minimum at the critical frequency, and then increases abruptly. As H_{rf} increases, the minimum H_{sw} decreases; namely, larger microwave assist effect is obtained. This switching behavior is similar to that reported for a single-layer perpendicular magnetic dot. After the abrupt increase, H_{sw} is still smaller than the intrinsic H_{sw} and then coincides with the intrinsic H_{sw}, as most obviously seen for $H_{rf} = 85$ Oe. This H_{sw} reduction after the primary MAS effect follows the trend depicted by the dashed line and can be attributed to the excitation of the higher-order FMR mode, which we show later by micromagnetic simulation.

Figure 7(b) shows H_{sw} vs f_{rf}, when a circularly polarized microwave field is generated by introducing a microwave signal to both CPWs. The rotation direction is mostly CW except for the plot depicted by crosses where the rotation direction is CCW. The results for $H_{rf} = 43$ Oe and 85 Oe coincide with those for $H_{rf} = 85$ Oe and 170 Oe in the linear polarization case. This coincidence is explained by the facts that a linearly polarized microwave field is the sum of CW and CCW circularly polarized microwave fields with half the field amplitude and that only the CW component induces MAS. As H_{rf} further increases, a larger MAS effect is obtained, and the slope of the $H_{sw} - f_{rf}$ curve changes at around 10 GHz. For $H_{rf} = 213$ Oe, a part of the HL magnetization first reverses, then the whole HL magnetization reverses in the f_{rf} range from 12 GHz to 14.5 GHz.[9] These nucleation and saturation fields are depicted by open circles and boxes in Fig. 7(b), respectively. The nucleation field shows a linear decrease with respect to f_{rf}, showing that the nucleation is induced by the HL excitation. On the other hand, the saturation field is the same regardless of f_{rf},
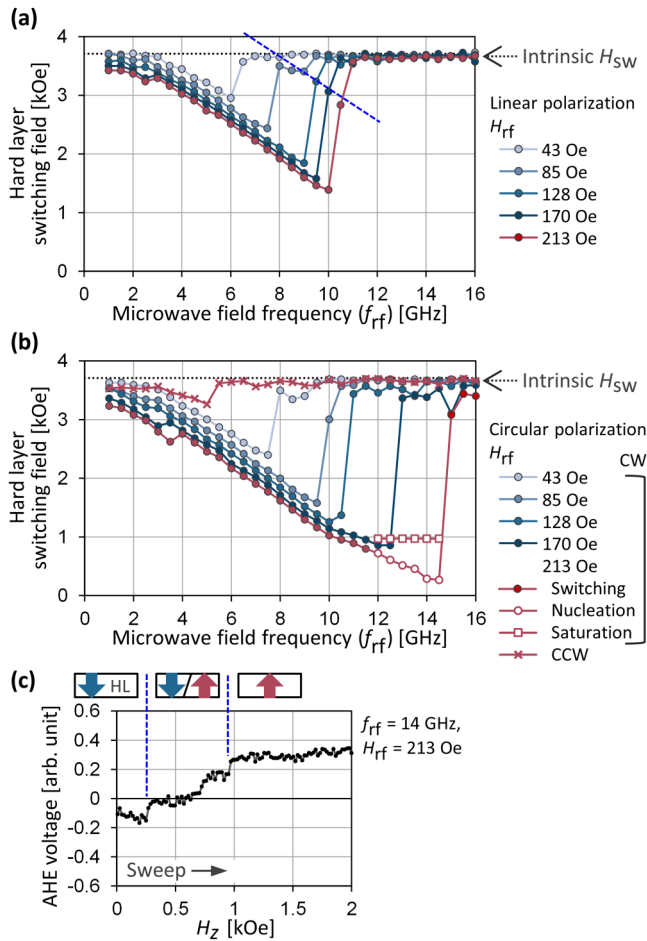
FIG. 7. (a) H_{sw} vs f_{rf} in the linearly polarized microwave field. The dashed line is guide for showing the H_{sw} reduction by excitation of the higher-order mode. (b) H_{sw} vs f_{rf} in the circularly polarized microwave field. The rotation direction of the microwave field is mostly CW except for the plot depicted by the crosses. The open circles and squares indicate the nucleation and saturation fields when nucleation-type switching is observed. (c) AHE voltage vs H_z in the circularly polarized microwave field for $f_{rf} = 14$ GHz and $H_{rf} = 213$ Oe. In this condition nucleation-type switching is observed.

showing that the saturation occurs as the reversed domain expands owing to H_z. Figure 7(c) shows AHE voltage vs H_z for nucleation-type switching. The AHE voltage shows multiple steps, and finally the HL magnetization saturates in the $+z$ direction at around $H_z = +1$ kOe. This result does not mean that magnetization switching scheme changes when large MAS effect is induced. Considering the size of the bilayer dot, magnetization switching is expected to occur as a reversed domain nucleates and expands. Only when H_{sw} decreases to $+1$ kOe by MAS, the reversed domain does not expand immediately and becomes detectable.

When the rotation direction is reversed to CCW, no obvious MAS effect is observed [crosses in Fig. 7(b)]. Note that the H_{sw} reduction at around $f_{rf} = 5$ GHz shows a similar trend to that in the

CW microwave fields, and is due to the CW component originating from the fact that the polarization of the microwave field is not perfectly circular. The MAS effect induced by the unintended CW component is smaller than that for $H_{rf} = 43$ Oe in Fig. 7(a), which is equivalent to $H_{rf} = 22$ Oe for circular polarization. This result means that the amplitude of the CW component is less than 22 Oe when the CCW microwave field with $H_{rf} = 213$ Oe is applied.

The AFC bilayer nanodot does not show obvious MAS effect in the CCW microwave field, and this result differs from that in Sec. III A, in which switching of HL occurs as a result of the SL excitation in the CCW microwave field. This difference is explained as follows. The reduction of H_{sw} indirectly induced by the SL excitation is smaller than that by the direct excitation of HL. Thus, the SL excitation needs to occur at H_z near the intrinsic H_{sw}. This condition is satisfied for the 500-nm sample at $f_{rf} = 10$ GHz, as shown in Fig. 4(c). On the other hand, for the 80-nm sample, f_{rf} to satisfy the condition increases because the patterning to the smaller size increases both intrinsic H_{sw} and SL FMR frequency. From micromagnetic simulation, we estimate that f_{rf} needs to be 20 GHz to excite the SL magnetization near the intrinsic H_{sw} (data not shown). When the SL FMR frequency is properly designed, H_{sw} reduction by the SL excitation is expected to occur for a nanodot sample. Although the microwave assist effect by the SL excitation is small, this switching scheme can be beneficial as in the following example. By employing MAS by SL excitation, the same HL can be used for multiple recording layers in multilayer recording. By changing the FMR frequency of SL of each recording layer, the SL excitation is induced layer-selectively by tuning f_{rf}, and accordingly layer-selective switching of HL is carried out.

Next, we apply a circularly polarized microwave field with time-varying frequency. The microwave field frequency is varied from a start frequency (f_{rf}^{start}) to $f_{rf}^{start}/2$ over a 10-ns duration according to the function $f_{rf}(t) = f_{rf}^{start} \exp[-(t/10) \cdot \ln(2)]$, where t denotes time in units of nanoseconds. This function was employed in Ref. 10, which reported that the rate of frequency change of this function is slow enough for the magnetization excitation to follow. Therefore, MAS behavior depends only on start and end frequencies, and the same result is expected for a different function unless the rate of frequency change is too fast. Figure 8 shows f_{rf}^{start} vs H_{sw}. In comparison with the constant-frequency case [Fig. 7(b)], the minimum H_{sw} achieved for $H_{rf} = 43$ Oe decreases from 2.4 kOe to 1.9 kOe, showing that the MAS effect is enhanced by applying the varying-frequency microwave field. At $f_{rf}^{start} = 16$ GHz, H_{sw} increases abruptly, which is explained as follows. To obtain MAS effect in a varying-frequency microwave field, the end frequency needs to be almost the same as the critical frequency for constant-frequency MAS.[10] At $f_{rf}^{start} = 16$ GHz, the end frequency is 8 GHz and larger than 7.5 GHz at which H_{sw} increases abruptly in Fig. 7(b). Thus, the primary MAS effect does not occur. Because the HL switching is still assisted by the excitation of the higher-order mode, H_{sw} is smaller than the intrinsic value. Enhancement of the MAS effect decreases as H_{rf} increases, and for $H_{rf} = 128$ Oe, the minimum H_{sw} becomes almost the same for the constant- and varying-frequency microwave field. This kind of behavior in which MAS enhancement decreases as H_{rf} increases has been reported for a single-layer perpendicular magnetic dot.[10]

The experimental results of MAS are analyzed by zero-temperature micromagnetic simulation. Figure 9(a) shows the dependence of the
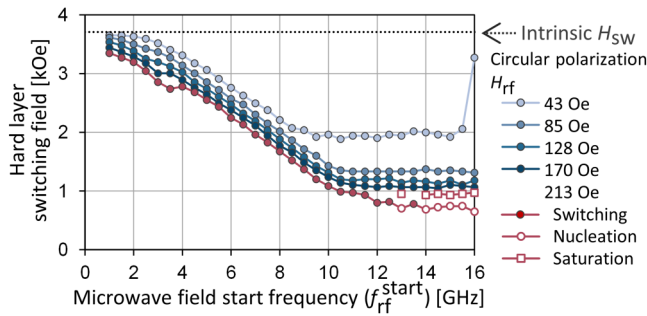
FIG. 8. H_{sw} vs f_{rf}^{start} in the circularly polarized microwave field with time-varying frequency. The microwave field varies from f_{rf}^{start} to $f_{rf}^{start}/2$ over a 10-ns time period.

normalized z-component magnetization $(0.75 \times m_z^{HL} + 0.25 \times m_z^{SL})$ on H_z. Similar to Fig. 5(a), the simulation result agrees with the experimental result except for H_{sw} because the simulation does not take account of thermal fluctuation. We focus on switching of HL from the antiferromagnetic configuration and obtain the dependence of H_{sw} on f_{rf} in a circularly polarized microwave field, as shown in
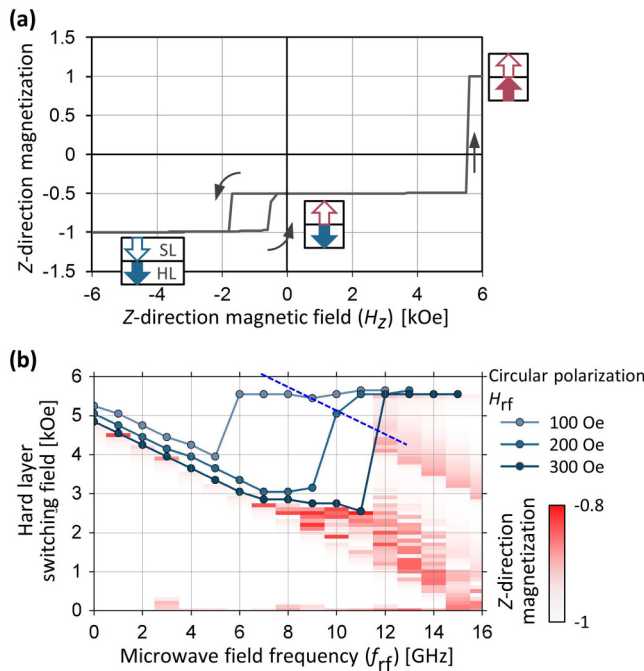

FIG. 9. (a) Computed normalized z-component magnetization $(0.75 \times m_z^{HL} + 0.25 \times m_z^{SL})$ vs H_z. Schematics depict the magnetization configuration. (b) computed H_{sw} vs f_{rf} in the circularly polarized microwave field. The dashed line is a guide for showing the H_{sw} reduction by the higher-order excitation mode. Magnetization excitation of HL for $H_{rf} = 300$ Oe is shown as a color plot in the background.

Fig. 9(b). As f_{rf} increases, H_{sw} gradually decreases and suddenly increases at the critical frequency, which agrees with the experimental result. In addition, two features—small H_{sw} reduction after the primary MAS effect depicted by the dashed line and change of the slope of the $H_{sw} - f_{rf}$ curve at $f_{rf} = 7$ GHz—are reproduced. Figure 8(b) also shows magnetization excitation of HL for $H_{rf} = 300$ Oe as a color plot in the background. When f_{rf} is below 7 GHz, magnetization switching occurs at the lower edge of the FMR linewidth. After the slope changes, the switching condition gradually enters the FMR linewidth. This kind of slope reduction has also been reported in MAS of a single-layer perpendicular magnetic dot, and it has been reported that the slope changes when MAS involves spatially non-uniform magnetization excitation.[6] The color plot also indicates a higher-order FMR mode. The H_{sw} reduction after the primary MAS
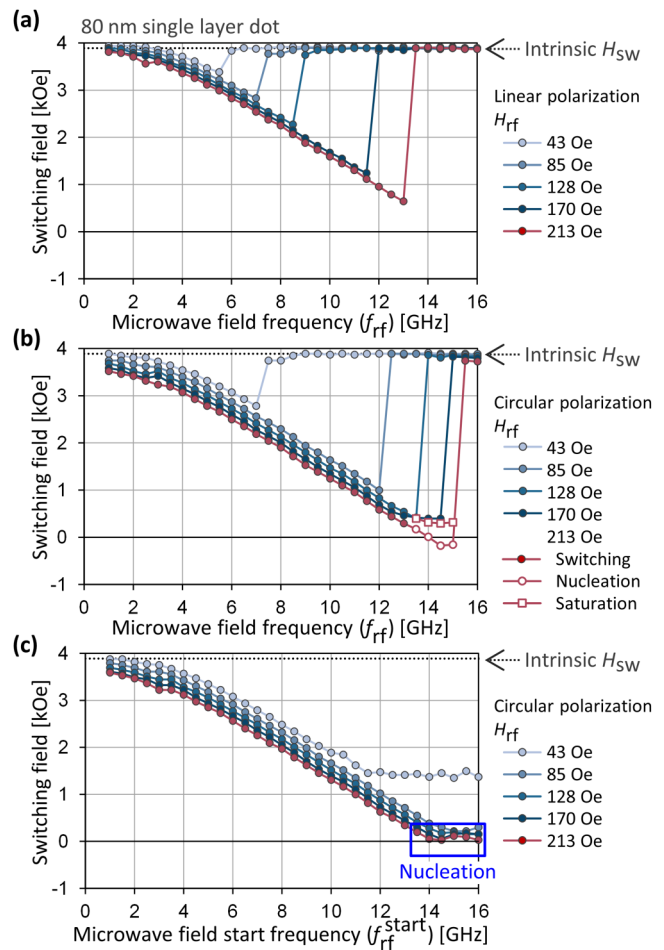

FIG. 10. (a) and (b) H_{sw} vs f_{rf} obtained for the single-layer perpendicular magnetic dot in the (a) linearly and (b) circularly polarized microwave field, respectively. (c) H_{sw} vs f_{rf}^{start} in the circularly polarized microwave field with time-varying frequency. When H_{rf} is 85 Oe and larger, nucleation-type switching is observed in the region depicted by the square. For clarity, only the nucleation fields are shown.

effect that appears in the experiment [Fig. 7(a)] can be explained by the excitation of this mode.

C. Comparison with microwave-assisted magnetization switching of a single-layer perpendicular magnetic dot

We investigate the MAS behavior of a single-layer perpendicular magnetic dot having the same size and almost the same H_{sw} as the AFC bilayer dot. Figures 10(a) and 10(b) show H_{sw} vs f_{rf} when a linearly polarized and circularly polarized microwave field is applied, respectively. Typical MAS behavior is obtained, and the result for the linearly polarized microwave fields coincides with that for the circularly polarized microwave fields with half the amplitude. Furthermore, nucleation-type switching is observed when H_{rf} becomes 213 Oe and H_{sw} decreases close to 0.5 kOe. The field at which nucleation-type switching is observed is smaller than in the case of the AFC bilayer dot, where H_{sw} needs to decrease close to 1 kOe. This difference in the field is due to the antiferromagnetic coupling field from SL. Figure 10(c) shows the dependence of H_{sw} on f_{rf}^{start}. The MAS effect is enhanced, and the minimum H_{sw} achieved for $H_{rf} = 43$ Oe decreases from 2.8 kOe to 1.4 kOe in comparison with the constant-frequency case. When H_{rf} is 85 Oe and larger, H_{sw} decreases close to 0 Oe, and nucleation-type switching is observed in the region shown by the box. The MAS behavior of the AFC bilayer dot and the single-layer magnetic dot shows these features in common, which demonstrates that MAS of the AFC bilayer occurs in the same manner and the antiferromagnetically coupled SL does not hinder the MAS effect.

IV. SUMMARY

In this paper, we fabricate an AFC bilayer consisting of two antiferromagnetically coupled magnetic layers with perpendicular magnetization and study the FMR excitation and magnetization switching behavior in a microwave field. AHE-FMR measurement in combination with a circularly polarized microwave field enables layer-selective analysis of the FMR excitation of the two magnetic layers. The linewidth of the FMR signal is broader in the antiferromagnetic configuration than in the ferromagnetic configuration, suggesting that the effective damping of the magnetic layer is larger in the antiferromagnetic configuration. The MAS behavior of the AFC bilayer dot exhibits the following features. H_{sw} decreases as the microwave field frequency increases and abruptly increases at the critical frequency, and a large H_{sw} reduction from approximately 4 kOe to 1 kOe is demonstrated. Nucleation-type switching is observed when H_{sw} decreases to less than 1 kOe by increasing H_{rf}. The enhancement of MAS is obtained by applying a microwave field with time-varying frequency. These features qualitatively coincide with those obtained for the single-layer perpendicular magnetic dot, showing that the AFC structure does not hinder the MAS effect.

ACKNOWLEDGMENTS

REFERENCES

[1] C. Thirion, W. Wernsdorfer, and D. Mailly, "Switching of magnetization by nonlinear resonance studied in single nanoparticles," Nature Mater. **2**, 524 (2003).

[2] J.-G. Zhu, X. Zhu, and Y. Tang, "Microwave assisted magnetic recording," IEEE. Trans. Magn. **44**, 125 (2008).

[3] J.-G. Zhu and Y. Wang, "Microwave assisted magnetic recording utilizing perpendicular spin torque oscillator with switchable perpendicular electrodes," IEEE. Trans. Magn. **46**, 751 (2010).

[4] I. Tagawa, M. Shiimoto, M. Matsubara, S. Nosaki, Y. Urakami, and J. Aoyama, "Advantage of MAMR read-write performance," IEEE Trans. Magn. **52**, 3101104 (2016).

[5] S. Okamoto, N. Kikuchi, M. Furuta, O. Kitakami, and T. Shimatsu, "Microwave assisted magnetic recording technologies and related physics," J. Phys. D: Appl. Phys. **48**, 353001 (2015).

[6] M. Furuta, S. Okamoto, N. Kikuchi, O. Kitakami, and T. Shimatsu, "Size dependence of magnetization switching and its dispersion of Co/Pt nanodots under the assistance of radio frequency fields," J. Appl. Phys. **115**, 133914 (2014).

[7] Y. Nozaki and S. Kasai, "Microwave-assisted magnetization reversal in exchange-coupled composite media using linearly polarized microwave fields," IEEE Tran. Magn. **52**, 3100207 (2016).

[8] H. Suto, T. Kanao, T. Nagasawa, K. Kudo, K. Mizushima, and R. Sato, "Subnanosecond microwave-assisted magnetization switching in a circularly polarized microwave magnetic field," Appl. Phys. Lett. **110**, 262403 (2017).

[9] H. Suto, T. Kanao, T. Nagasawa, K. Mizushima, and R. Sato, "Zero-dc-field rotation-direction-dependent magnetization switching induced by a circularly polarized microwave magnetic field," Sci. Rep. **7**, 13804 (2017).

[10] H. Suto, T. Kanao, T. Nagasawa, K. Mizushima, and R. Sato, "Magnetization switching of a Co / Pt multilayered perpendicular nanomagnet assisted by a microwave field with time-varying frequency," Phys. Rev. Appl. **9**, 054011 (2018).

[11] Y. Nakayama, Y. Kusanagi, T. Shimatsu, N. Kikuchi, S. Okamoto, and O. Kitakami, "Microwave-assistance effect on magnetization switching in antiferromagnetically coupled CoCrPt granular media," IEEE Trans. Magn. **52**, 3201203 (2016).

[12] S. Greaves, Y. Kanai, and H. Muraoka, "Antiferromagnetically coupled media for microwave-assisted magnetic recording," IEEE Trans. Magn. **54**, 3000111 (2018).

[13] G. Winkler, D. Suess, J. Lee, J. Fidler, M. A. Bashir, J. Dean, A. Goncharov, G. Hrkac, S. Bance, and T. Schrefl, "Microwave-assisted three-dimensional multilayer magnetic recording," Appl. Phys. Lett. **94**, 232501 (2009).

[14] S. Li, B. Livshitz, H. N. Bertram, E. E. Fullerton, and V. Lomakin, "Microwave-assisted magnetization reversal and multilevel recording in composite media," J. Appl. Phys. **105**, 07B909 (2009).

[15] H. Suto, T. Nagasawa, K. Kudo, T. Kanao, K. Mizushima, and R. Sato, "Layer-selective switching of a double-layer perpendicular magnetic nanodot using microwave assistance," Phys. Rev. Appl. **5**, 014003 (2016).

[16] Y. Li, S. Okamoto, N. Kikuchi, O. Kitakami, and T. Shimatsu, "Layer-selective microwave-assisted magnetization switching in a dot of double antiferromagnetically coupled (AFC) layers," Appl. Phys. Lett. **112**, 162404 (2018).

[17] E. N. Abarra, A. Inomata, H. Sato, I. Okamoto, and Y. Mizoshita, "Longitudinal magnetic recording media with thermal stabilization layers," Appl. Phys. Lett. **77**, 2581 (2000).

[18] E. E. Fullerton, D. T. Margulies, M. E. Schabes, M. Carey, B. Gurney, A. Moser, M. Best, G. Zeltzer, K. Rubin, H. Rosen, and M. Doerner, "Antiferromagnetically coupled magnetic media layers for thermally stable high-density recording," Appl. Phys. Lett. **77**, 3806 (2000).

[19] E. Girt and H. J. Richter, "Antiferromagnetically coupled perpendicular recording media," IEEE. Trans. Magn. **39**, 2306 (2003).

[20] S. N. Piramanayagam, K. O. Aung, S. Deng, and R. Sbiaa, "Antiferromagnetically coupled patterned media," J. Appl. Phys **105**, 07C118 (2009).

[21] M. Ranjbar, S. N. Piramanayagam, D. Suzi, K. O. Aung, R. Sbiaa, Y. S. Kay, S. K. Wong, and C. T. Chong, "Antiferromagnetically coupled patterned media and control of switching field distribution," IEEE. Trans. Magn. **46**, 1787 (2010).

[22]S. S. P. Parkin, N. More, and K. P. Roche, "Oscillations in exchange coupling and magnetoresistance in metallic superlattice structures: Co/Ru, Co/Cr, and Fe/Cr," Phys. Rev. Lett. **64**, 2304 (1990).

[23]K. Yakushiji, A. Sugihara, A. Fukushima, H. Kubota, and S. Yuasa, "Very strong antiferromagnetic interlayer exchange coupling with iridium spacer layer for perpendicular magnetic tunnel junctions," Appl. Phys. Lett. **110**, 092406 (2017).

[24]H. Suto, T. Nagasawa, K. Kudo, K. Mizushima, and R. Sato, "Nanoscale layer-selective readout of magnetization direction from a magnetic multilayer using a spin-torque oscillator," Nanotechnology **25**, 245501 (2014).

[25]T. Kanao, H. Suto, K. Kudo, T. Nagasawa, K. Mizushima, and R. Sato, "Transient magnetization dynamics of spin-torque oscillator and magnetic dot coupled by magnetic dipolar interaction: Reading of magnetization direction using magnetic resonance," J. Appl. Phys. **123**, 043903 (2018).

[26]Y. Nakamura, M. Nishikawa, H. Osawa, Y. Okamoto, T. Kanao, and R. Sato, "Envelope detection using temporal magnetization dynamics of resonantly interacting spin-torque oscillator," AIP Adv. **8**, 056512 (2018).

[27]T. Kanao, H. Suto, K. Mizushima, and R. Sato, "Layer-selective detection of magnetization directions from two layers of antiferromagnetically-coupled magnetizations by ferromagnetic resonance using a spin-torque oscillator" (unpublished).

[28]N. Kikuchi, M. Furuta, S. Okamoto, O. Kitakami, and T. Shimatsu, "Quantized spin waves in single Co/Pt dots detected by anomalous hall effect based ferromagnetic resonance," Appl. Phys. Lett. **105**, 242405 (2014).

[29]A. Vansteenkiste, J. Leliaert, M. Dvornik, M. Helsen, F. Garcia-Sanchez, and B. V. Waeyenberge, "The design and verification of MuMax3," AIP Adv. **4**, 107133 (2014).

[30]S. V. Vonsovskii, *Ferromagnetic Resonance* (Pergamon, New York, 1966).

[31]J. Xu, V. Sluka, B. Kardasz, M. Pinarbasi, and A. D. Kent, "Ferromagnetic resonance linewidth in coupled layers with easy-plane and perpendicular magnetic anisotropies," J. Appl. Phys. **124**, 063902 (2018).

[32]K. Tanaka, T. Moriyama, M. Nagata, T. Seki, K. Takanashi, S. Takahashi, and T. Ono, "Linewidth broadening of optical precession mode in synthetic antiferromagnet," Appl. Phys. Express **7**, 063010 (2014).